Full title: Vaccine-linked chemotherapy with a low dose of benznidazole plus a bivalent recombinant protein vaccine prevents the development of cardiac fibrosis caused by *Trypanosoma cruzi* in BALB/c mice.

Short title: Vaccine-linked chemotherapy prevents cardiac fibrosis.

Victor Manuel Dzul-Huchim[1], Maria Jesus Ramirez-Sierra[1], Pedro Pablo Martinez-Vega[1], Miguel Enrique Rosado-Vallado[1], Victor Ermilo Arana-Argaez[2], Jaime Ortega-Lopez[3], Fabian Gusovsky[4], Eric Dumonteil[5], Julio Vladimir Cruz-Chan[1], Peter Hotez[6,7], María Elena Bottazzi[6,7] and Liliana Estefania Villanueva-Lizama[1]*

[1]Laboratorio de Parasitología, Centro de Investigaciones Regionales Dr. Hideyo Noguchi, Universidad Autónoma de Yucatán, Mérida, Yucatán, México

[2]Laboratorio de Farmacología, Facultad de Química, Universidad Autónoma de Yucatán, Mérida, Yucatán, México

[3]Departamento de Biotecnología y Bioingeniería, Centro de Investigación y Estudios Avanzados del Instituto Politécnico Nacional, Ciudad de México, México

[4]Eisai, Inc., Eisai Inc, Andover, Massachusetts, United States of America

[5]Department of Tropical Medicine, School of Public Health and Tropical Medicine, and Vector-Borne and Infectious Disease Research Center, Tulane University, New Orleans, Los Angeles, United States of America

[6]Texas Children's Center for Vaccine Development, Departments of Pediatrics and Molecular Virology & Microbiology, Baylor College of Medicine, Houston, Texas, United States of America.

[7]Department of Biology, Baylor University, Waco, Texas, United States of America.

***Corresponding author:**

liliana.villanueva@correo.uady.mx

Abstract

Background

Chagas disease (CD) is caused by *Trypanosoma cruzi* and affects 6-7 million people worldwide. Approximately 30% of chronic patients develop chronic chagasic cardiomyopathy (CCC) after decades. Benznidazole (BNZ), one of the first-line chemotherapy approved for CD, induces toxicity and fails to halt the progression of CCC in chronic patients. The recombinant parasite-derived antigens, including Tc24, Tc24-C4, TSA-1, and TSA-1-C4 with Toll-like receptor 4 (TLR-4) agonist-adjuvants reduce cardiac parasite burdens, heart inflammation, and fibrosis, leading us to envision their use as immunotherapy together with BNZ. Given genetic immunization (DNA vaccines) encoding Tc24 and TSA-1 induce protective immunity in mice and dogs, we propose that immunization with the corresponding recombinant proteins offers an alternative and feasible strategy to develop these antigens as a bivalent human vaccine. We hypothesized that a low dose of BNZ in combination with a therapeutic vaccine (TSA-1-C4 and Tc24-C4 antigens formulated with a synthetic TLR-4 agonist-adjuvant, E6020-SE) could provide antigen-specific T cell immunity and prevent cardiac fibrosis progression.

Methodology/ Principal findings

We evaluated the therapeutic vaccine candidate plus BNZ (25 mg/kg/day/7 days) given at days 72 and 79 post-infection (p.i) (early chronic phase). Fibrosis, inflammation, and parasite burden were quantified in heart tissue at day 200 p.i. (late chronic phase). Further, spleen cells were collected to evaluate antigen-specific $CD4^+$ and $CD8^+$ T cell immune responses, using flow cytometry. We found that vaccine-linked BNZ treated mice had lower cardiac fibrosis compared to the infected untreated control group. Moreover, cells from mice that received the immunotherapy had higher stimulation index of antigen-specific $CD8^+Perforin^+$ T cells as well as antigen-specific central memory T cells compared to infected untreated control.

Conclusions

Our results suggest that the bivalent immunotherapy together with BNZ treatment protects mice against cardiac fibrosis and activates strong $CD8^+$ T cell responses by *in vitro* restimulation, evidencing the induction of a long-lasting *T. cruzi*-immunity.

Author summary

Chagas disease (CD) is a neglected tropical disease caused by the parasite *Trypanosoma cruzi,* transmitted through contact with infected feces of vectors bugs. CD can induce cardiac abnormalities including the development of fibrosis and eventually death. Benznidazole (BNZ) is the first-line drug approved against CD, however, its toxicity and lack of efficacy in the chronic phase have limited its use. Previous studies have demonstrated the feasibility

of reducing doses of BNZ given in combination with therapeutic vaccines during the acute phase of CD, which increases its tolerability and reduces adverse side effects. Considering that patients are often diagnosed until prolonged stages of the disease, its necessary to evaluate therapies given in the chronic phase of CD. In this study, we evaluated a vaccine formulated with the recombinant *T. cruzi*-antigens TSA-1-C4 and Tc24-C4 and the adjuvant E6020-SE in combination with a low dose of BNZ given during the chronic phase of *T. cruzi*-infection using a murine model. The authors found that the combination therapy protects mice against cardiac fibrosis, allow the activation of a $CD8^+$ T cell response and induce a prolonged memory response against *T. cruzi*. This study supports the development of the vaccine-linked chemotherapy approach in order to prevent *T. cruzi* chronic infection.

Introduction

Chagas disease (CD) is caused by the protozoan parasite *Trypanosoma cruzi* (*T. cruzi*) transmitted mainly through contact with infected feces of hematophagous triatomine bugs. CD affects approximately 6.5 million people worldwide and is a major public health problem in Latin America (1). Moreover, CD is emerging in non-endemic regions due to human migration, political and socioeconomic instability, climate change and other factors (2). CD has two major clinical stages. The first is the acute infection and is characterized by high levels of parasites in peripheral blood; where individuals are mostly asymptomatic but can present non-specific febrile illness, which typically resolves within 4–8 weeks (3,4). In the chronic phase, where approximately 20-30% of individuals develop chronic chagasic

99 cardiomyopathy (CCC) years to decades after the initial infection, and some develop
100 pathologies such as megaesophagus and megacolon (5,6). The pathogenesis of CCC is due
101 to *T. cruzi* persistence in the heart that drives chronic inflammation and fibrosis leading to
102 abnormalities of the conduction system, e.g., right bundle branch block (RBBB),
103 arrhythmias, tachycardia and subsequently death by heart failure (4,7,8). Benznidazole
104 (BNZ), is one of the first-line chemotherapies used for CD treatment, however, it is
105 associated with toxic side effects, has a poor efficacy in patients with chronic infection and
106 they require long treatment, increasing the risk of drug resistance (9). Furthermore, therapy
107 with BNZ does not reduce cardiac clinical deterioration through 5 years of follow-up in CCC
108 patients (10). Conversely, other studies have reported that BNZ treatment is associated with
109 a reduction in heart disease progression, suggesting that more trials focused on BNZ should
110 be performed (11). The contrasting results between these studies may be explained by several
111 factors as the number of individuals evaluated in each study, differences of geographical area
112 where individuals are from, variation of parasite strains causing the infection, rates of loss to
113 follow-up, and the diversity of clinical status of enrolled patients

114 The immune response required to reduce parasite dissemination, prevent cardiac
115 lesions, and ensure host survival against *T. cruzi*, is still under investigation. The
116 development and use of therapeutic vaccines are an alternative approach against CD. Its
117 purpose is to stimulate the immune response from the host against *T. cruzi*-infection. Several
118 therapeutic vaccine candidates have been evaluated exploring a vast of delivery systems
119 (plasmids, adenoviruses, peptides and recombinant proteins) and adjuvants (12–16). Overall,
120 in animal models of *T. cruzi* experimental infection, either T helper (Th)-1 or Th1/Th2
121 balanced and Th-17 immune responses are required to achieve parasite control (17–19) with

122 evidence for the importance of IFNγ and $CD8^+$ T cells (20,21). A protective immunity is
123 mediated by $CD8^+$ cytolytic T cells (CTL), which release cytotoxic granules (perforin and
124 granzymes) (21,22). Perforin is a pore forming cytolytic protein, that allows the transition of
125 granzymes, a group of serine proteases, which induce programmed cell death in *T. cruzi*
126 infected cells (23,24). In addition, $CD8^+$ T cells modulate the immune response through the
127 secretion of pro-inflammatory cytokines, such as IFNγ, IL-12 and tumor necrosis factor alpha
128 (TNF-α) (25–27).

129 Our program has been examining the effects of two major recombinant protein
130 antigens, together with Toll-like receptor 4 (TLR-4) agonist adjuvants. These antigens
131 include a flagellar calcium-binding protein, Tc24, or a genetically re-engineered Tc24
132 antigen with cysteine modifications to prevent aggregation, known as Tc24-C4 (28,29), and
133 a trypomastigote surface antigen known as TSA-1 (30). Hence, both proteins are being
134 produced under current good manufacturing practices (cGMP) as potential vaccines. Studies
135 performed in acute *T. cruzi*-infection in mice indicate that both Tc24 and TSA-1 recombinant
136 proteins drive a Th1 or balanced Th1/Th2 immunity in achieving therapeutic effects, with an
137 emphasis on their role in reducing parasite persistence in the heart, and the associated with
138 fibrosis and inflammation (15–17,31,32). To date, most of the studies in mice have focused
139 on immunizations using a single recombinant protein antigen, nevertheless our earlier work
140 using plasmid DNA immunization evaluating bivalent vaccines with both TSA-1 and Tc24
141 (33), demonstrated that there is a beneficial effect to use bivalent vaccines when are
142 administered in mice during acute infection.

143 In addition, studies focused on evaluating the phenotype of memory T cells are
144 important for vaccine development; identification of a vaccine that can effectively induce

lasting memory-response is expected to prevent infection. According to the model proposed by Lanzavecchia and Sallusto (34), based on the expression of receptors required for lymph node homing, memory T cells are often classified as central memory (T_{CM}), which can migrate to inflamed peripheral tissues and display immediate effector function, or effector memory (T_{EM}) which remain in secondary lymphoid organs, have little or no effector function, but readily proliferate and differentiate to effector cells. Therefore, therapeutic vaccination strategies have focused on promoting antigen-specific $CD4^+$ and $CD8^+$ memory T cells during the chronic phase of *T. cruzi*-infection (35–38), which is also when most Chagasic patients seek treatment.

On the other hand, BNZ dosage and treatment regimens have been controversial in recent years. To assess the feasibility of minimizing the toxic side-effects, several trials have been performed to test low doses of BNZ given alone or in combination with other drugs or antigens (39–41). Accordingly, combined regimens improve the trypanocide activity and attenuate the BNZ toxicity, thus, these studies support the evaluation of an immunotherapy based on a reduced low-dose of BNZ linked to a vaccine formulated with the recombinant proteins TSA-1-C4 and Tc24-C4. Recently studies have demonstrated the efficacy of the recombinant Tc24-C4 antigen in combination with a low dose of BNZ administered during *T. cruzi* acute infection in a murine model resulting in increased antigen-specific $CD8^+$ and IFNγ-producing $CD4^+$ T cells populations, as well as in increased cytokines related to Th17 immune responses (42).

Although the bivalent vaccine has shown immunogenicity and protection in acute murine models, it needs to be evaluated in pre-clinical models of *T. cruzi* chronic infection. Hence, our group previously performed a pilot study in order to evaluate the progression of

168 *T. cruzi* chronic infection in BALB/c mice based on the parasitemia and cardiac clinical
169 manifestations evaluated using electrocardiograms (taken every 35 days) and
170 echocardiograms (at 210 dpi). Those results suggested that days 72 and 200 p.i. were
171 representative time points of the early and late phases of chronic infection, respectively
172 (manuscript in preparation).

173 In this study, we evaluated an immunotherapy administrated during the early
174 chronic phase of experimental *T. cruzi* infection. We hypothesized that a low dose BNZ
175 treatment in combination with a therapeutic vaccine (TSA-1-C4 and Tc24-C4 recombinant
176 antigens in a formulation with a synthetic TLR-4 agonist-adjuvant, E6020-SE) could provide
177 a strong antigen-specific $CD8^+$ T cell immunity, improving memory response and preventing
178 the development of cardiac fibrosis.

179 This study could support the use of the vaccine-linked chemotherapy approach given
180 in early chronic infection, preventing or delaying the development of severe manifestations
181 in prolonged stages of CD.

182

183 Materials and methods

184 Ethics statements

185 All studies were approved by the institutional bioethics committee of the "Centro de
186 Investigaciones Regionales Dr. Hideyo Noguchi", Universidad Autónoma de Yucatán
187 (Reference #CEI-08-2019) and were performed in strict compliance with NOM-062-ZOO-
188 1999.

Proteins, adjuvant and benznidazole

The recombinant TSA-1-C4 and Tc24-C4 antigens were obtained from the Centro de Investigación y Estudios Avanzados (CINVESTAV) of the Instituto Politécnico Nacional (IPN), Mexico. Each TSA-1-C4 or Tc24-C4 coding sequence was cloned into a pET41a+ *E. coli* expression vector. The resulting plasmid DNA was transformed into BL21 (DE3) cells induced with isopropyl-beta-D-1-thiogalactoside (IPTG) for protein expression. Recombinant proteins were purified by ion exchange (IEX) and size exclusion chromatography (SEC) (28,30). The integrity and size of each recombinant protein were analysed by SDS-PAGE electrophoresis (**S1 Fig**). The recombinant proteins were formulated with the adjuvant E6020 in a stable squalene emulsion (SE). E6020 Toll-like receptor 4 agonist was acquired through Eisai, Inc (43). Benznidazole (N-Benzyl-2-nitro-1H-imidazole-1-acetamide) was obtained through Sigma Aldrich®; for its use, it was solubilized in 5% dimethyl sulfoxide (DMSO)-95% deionized water (32,42).

Mice and parasites

Female BALB/c mice (BALB/cAnNHsd) were obtained at 3-4 weeks old from ENVIGO-Mexico. Animals were housed in groups of 5 per cage, received *ad libitum* food and water and a 12-h light/dark cycle. Mice were acclimated for two weeks before starting the study. *T. cruzi* H1 parasites, originally isolated from a human case in Yucatan, Mexico were maintained by serial passage in BALB/c mice every 25 to 28 days and used for infections as previously described (44).

Macrophages cell line

RAW 264.7 cell line was acquired from American type culture collection (ATCC® TIB-71™). Cells were cultured in DMEM medium (Gibco ®) supplemented with 10% fetal bovine serum (FBS, Gibco ®) and 1% penicillin/streptomycin (Gibco ®), in an atmosphere of 5% CO_2 and 95% humidity at 37 ºC. Cells were passaged in T-75 culture flasks (Corning ®) after reaching 80% confluence and were detached using 0.25% trypsin (Corning ®).

Experimental infection and therapeutic treatment

A total of 70 mice were infected with 500 trypomastigotes of *T. cruzi* (H1 strain) by intraperitoneal injection. In order to confirm the infection, parasitemia was measured in Neubauer chamber by examination of fresh blood collected from the mouse tail at day 27 post-infection. (**S1 Table**). Survival was monitored up to day 200 post-infection (p.i) (**S2 Fig**). At day 72 p.i. (early chronic phase) surviving mice were randomly divided into groups of 8 individuals, the therapeutic vaccine was injected intramuscularly, and a vaccine boost with the same formulation was administrated one week after (day 79 p.i.). Each vaccine dose consisted of 12.5 µg of recombinant TSA-1-C4, 12.5 µg of recombinant Tc24-C4 and 5 µg of E6020-SE (28,32). From day 72 to 79 p.i., mice were given daily 25 mg/kg BNZ by oral gavage, which corresponds to a 4-fold reduction in the conventional regimen of BNZ treatment. Additional groups of mice received the therapeutic vaccine alone (12.5 µg of TSA-1-C4, 12.5 µg of Tc24-C4 and 5 µg of E6020-SE), low dose BNZ alone (25 mg/kg), E6020-SE alone (5 µg) or saline solution as control. Groups that did not receive BNZ were given the vehicle solution (5% DMSO in 95% deionized water) by oral gavage. One additional control group with four non-infected mice was also included. At day 200 p.i., mice were

231 euthanized using ketamine/xylazine-induced deep anaesthesia followed by cervical
232 dislocation, and spleens and hearts were collected for further analysis (**Fig 1**).

233

234 **Fig 1. Timeline for experimental infection, prime-boost vaccination and euthanize using**
235 **murine model.**

236

237 Quantification of parasites burden

238 Total DNA was isolated from cardiac tissue using the Kit Wizard® Genomic DNA
239 purification (Promega Madison WI). Each sample was quantified employing a BioSpec-nano
240 spectrophotometer system (SHIMADZU®) and adjusted to 50 ng of DNA from cardiac
241 tissue, then quantitative real-time PCR (qPCR) was performed in an Illumina® EcoTM
242 thermocycler using SYBR Green Master Mix® 1X and primers TCZ-F 5'-
243 GCTCTTGCCCACAMGGGTGC-3' and TCZ-R 5'-CCAAGCAGCGGATAGTTCAGG-3,
244 which amplify a 188 pb product from the satellite region of *T. cruzi* DNA (45,46). Cardiac
245 parasite burdens were calculated based on a standard curve and expressed as parasite
246 equivalents per 50 ng *T. cruzi*-DNA (47).

247 Cardiac fibrosis and inflammation

248 For histopathological analysis, cardiac tissue from euthanized mice was fixed in 10% neutral
249 buffered formalin solution, embedded in paraffin, cut into 5 µm sections, and stained with
250 either Masson's trichrome or haematoxylin and eosin (H&E) for fibrosis or inflammation

infiltrate measurement respectively. To assess cardiac fibrosis or cardiac inflammation, five representative pictures from each slide stained were acquired at 10X magnification using an OLYMPUS microscope (CX23) adapted with a digital camera MiniVID P/N TP605100 (LW Scientific ®). Image analysis was performed using ImageJ software version 2.0.0/1.52p. To quantify cardiac fibrosis, pixels corresponding to fibrosis (blue coloured) were quantified and normalized by subtracting the average data obtained from non-infected control group to total pixels of the sample to assess the percentage of fibrotic area in the cardiac tissue (16,42,48). To quantify inflammatory infiltrate, the number of pixels corresponding to total nuclei was quantified and normalized to total cardiac tissue area (48,49). Data is presented as cardiac fibrosis percentage area or cardiac inflammatory cells per mm^2.

Preparation of spleen mononuclear cells

Spleens were mechanically dissociated by being pressed through a 100 µm pore-size cell strainer. Splenocytes were rinsed with RPMI medium (Gibco ®) supplemented with 10% FBS and 1% penicillin-streptomycin (RPMIc) and pelleted by centrifugation for 5 min at 400 x *g* at room temperature. The supernatant was decanted, and the splenocyte pellet was resuspended in balanced salt solution buffer (BSS) pH 7.4. Afterwards, the splenocyte suspension was mixed with Ficoll-histopaque (GE Healthcare BIO-Sciences®) solution in 3:4 proportion and centrifuged at 400 x *g* for 40 min. The mononuclear cell layer was collected and washed twice with BSS buffer. The cell pellet was resuspended in RPMIc medium, cell viability was assessed by Trypan blue exclusion test and cell numbers were determined in a Neubauer chamber.

Intracellular cytokine and memory T cell immune phenotyping

A total of $5x10^5$ mononuclear cells were co-cultivated with RAW 264.7 macrophages previously stimulated with TSA-1-C4+Tc24-C4 (25 µg/mL final concentration) in 10:1 proportion. Co-cultures were incubated in 5% CO_2 and 95% humidity at 37ºC during 20 h for intracellular cytokine production or 96 h for memory immune-phenotyping assays. To evaluate intracellular cytokine production, brefeldin A (BD biosciences ®) was added to co-culture for the last 4 hours of incubation. Re-stimulated cells were collected and washed twice with PBS+BSA 0.01%, then, cells were stained with anti-CD3 Alexa-647 (BD biosciences ®), anti-CD4 PE-Cy7 (BD biosciences ®) and anti-CD8 PERCP-Cy5.5 (BD biosciences ®) (30) or anti-CD3 PE-Cy7 (BD biosciences®), anti-CD4 APC (BD biosciences ®), anti-CD8 BB515 (BD biosciences ®), anti-CD44 PE (BD biosciences ®) and anti-CD62L BV510 (BD biosciences ®) for memory immune-phenotyping assay. For intracellular cytokine production, cells were fixed with Cytofix/Cytoperm (BD biosciences ®), and permeabilized according to the manufacturer's instructions. Permeabilized cells were stained with anti-IFNγ (BD biosciences ®) and anti-Perforin (INVITROGEN ®). Cells were resuspended in FACS buffer and acquired on a BD FACSVerse flow cytometer. At least 50,000 total events in the mononuclear cell gate were obtained using FACSuite™ software version 1.0.5. Data were analysed in FlowJo software version 10.0.7r2. Stimulation index was calculated with the frequency of cells (stimulated with TSA-1-C4+Tc24-C4) and the frequency of non-stimulated cells (RPMIc alone). For intracellular analysis, stimulation index was measured with the median fluorescent intensity (MFI) of stimulated cells and the MFI of non-stimulated cells. A stimulation index > 1, indicates the presence of antigen-specific cells. Flow cytometry gating strategies for IFNγ and perforin expression or memory responses are presented in **S3 Fig** and **S4 Fig**.

Statistical analysis

All tests were run in GraphPad Prism software version 6.0.c. Data were analysed by one-way ANOVA or Kruskal–Wallis tests for multiple groups, depending on its distribution followed by Tukey or Dunn's *post hoc* test. When only two comparison groups were analysed, Student´s t-test or Mann–Whitney U-test was performed depending on data distribution. Differences between groups were considered statistically significant when *P*-value was less than 0.05.

Results

Vaccine-linked chemotherapy administered during the early chronic infection prevents cardiac fibrosis caused by *T. cruzi*

To evaluate the therapeutic efficacy of the vaccine-linked treatment, we measured cardiac *T. cruzi*-parasite burden, fibrosis, and inflammation. At day 200 p.i. *T. cruzi* cardiac parasite burden from mice treated and untreated was below the limit of detection of our qPCR test (<1 parasite per 50 ng of cardiac tissue) (**Fig 2A**). There were no differences comparing all experimental groups (Kruskal-Wallis, *P*=0.054). These data suggest that the methodology used has limitations in determining the therapeutic efficacy upon burden parasite of the formulation during the late chronic phase of infection in BALB/c mice.

316 **Fig 2. Protective effect of the vaccine-linked chemotherapy.** Mice were euthanized at day
317 200 p.i and heart samples were collected. (**A**) Cardiac parasite burdens were quantified by
318 quantitative real-time PCR. The dotted line represents the cut-off for the limit of detectable
319 quantification (LOQ) based on serially diluted *T. cruzi*-enriched cardiac tissue DNA (1
320 parasite equivalents per 50 ng of DNA). Each point represents an individual mouse;
321 horizontal lines denote median ± interquartile ranges values; significance calculated by
322 Kruskal-Wallis test with Dunn's correction for multiple comparisons. (**B**) Percentage fibrosis
323 area in non-infected and infected untreated mice. Bars denote means and standard deviation;
324 significance calculated by Student´s t-test. (**C**) Percentage fibrosis area for all experimental
325 groups. The cardiac fibrosis was quantified from representative images of Masson´s
326 trichrome-stained tissue sections using Image J software. Each point represents an individual
327 mouse, horizontal lines denote means ± SD; significance was calculated by Student´s t-test.
328 (**D**) Infiltrate cells/mm^2 in non-infected and infected untreated mice. Bars denote means and
329 standard deviation; significance calculated by Student´s t-test. (**E**) Infiltrate cells/mm^2 for all
330 experimental groups. Cardiac inflammation was quantified from representative images of
331 H&E-stained tissue sections using Image J software. Each point represents an individual
332 mouse, horizontal lines denote median ± interquartile ranges values; significance was
333 calculated by Mann-Whitney U-test. Significance is indicated as follows *, $P \leq 0.05$; **,
334 $P \leq 0.01$; ***, $P \leq 0.001$.

335

336 On the other hand, we evaluated cardiac fibrosis in heart tissue sections collected
337 from *T. cruzi*-infected mice at day 200 p.i. Representative images of Masson´s trichrome
338 stained-cardiac tissue from each experimental group are shown in **Fig 3A-F**. As we observed

in **Fig 2B**, there was a significantly higher percentage of cardiac fibrosis in infected untreated mice (2.426 ± 0.51) compared to non-infected mice (1.259 ± 0.299) (Student´s t-test, P=0.003). Thus, mice infected with *T. cruzi* developed cardiac fibrosis as a consequence of chronic infection. Also, we found significant differences comparing the combination of low BNZ + vaccine (0.551 ± 0.223) with infected untreated mice (1.167 ± 0.510) or low BNZ alone treated mice (1.889 ± 1.065) (Student´s t-test, P=0.012 and P=0.006 respectively) (**Fig 2C**). This finding suggests that the vaccine-linked chemotherapy administered at early chronic infection prevents cardiac fibrosis caused by *T. cruzi* chronic infection. On the other hand, we observed significantly lower fibrosis percentage in vaccine alone treated mice (0.784 ± 0.573) compared to low BNZ alone group (Student´s t-test, P=0.029), suggesting that the use of the vaccine (TSA-1-C4+Tc24-C4+E6020-SE) is better than BNZ treatment at lower dose in our experimental infection model (**Fig 2C**).

Fig 3. Representative images of Masson´s trichrome stained-cardiac tissue from (**A**) non-infected, (**B**) infected untreated, (**C**) E6020-SE, (**D**) low BNZ, (**E**) Vaccine and (**F**) low BNZ plus vaccine experimental groups. Cardiac muscle appears in red and collagen fibbers in blue. Black arrows show collagen staining.

We also evaluated the inflammatory infiltrate in heart tissue sections collected from *T. cruzi*-infected mice at day 200 p.i. Representative images of H&E stained-cardiac tissue from the different experimental groups are shown in **Fig 4A-F**. According to **Fig 2D** we observed similar levels of inflammatory cell density between non-infected mice (2,143 ±

265.1) and infected untreated mice (2,329 ± 302.9), (Student´s t-test, P=0.335). Hence, our findings suggest that infected mice at late chronic infection (200 days p.i.) present basal levels of infiltrating inflammatory cells. Moreover, a significantly lower proportion of infiltrating inflammatory cells was found comparing infected untreated mice with E6020-SE alone (1290 ± 636.4) or low BNZ alone (1485 ± 223.7) groups (Mann-Whitney U-test, P=0.002 and P<0.001 respectively) (**Fig 2E**), suggesting that, using this experimental infection model, either adjuvant or BNZ treatments given alone contributes to the development of cardiac inflammation. Interestingly, we observed that the low BNZ + vaccine-treated group (537.5 ± 820.9) had significantly lower levels of inflammatory cell density compared to low dose BNZ-treated group (Mann-Whitney U-test, P=0.04) (**Fig 2E**), indicating that there is a benefit adding the vaccine formulation to the BNZ alone treatment.

Fig 4. Representative images of H&E stained-cardiac tissue from (**A**) non-infected, (**B**) infected untreated, (**C**) E6020-SE, (**D**) low BNZ, (**E**) Vaccine and (**F**) low BNZ plus vaccine experimental groups. Cardiac muscle appears in pink and the nuclei of infiltrating inflammatory cells appear in purple. Black arrows show the presence of infiltrating inflammatory cells.

Immunotherapy with low BNZ plus vaccine primes a cytotoxic profile in $CD8^+$ and $CD4^+$ T antigen-specific cells

We evaluated the presence of antigen-specific $CD4^+$ and $CD8^+$ T cells in mice during the late chronic infection. As shown in **S5 Fig**, all experimental groups had a mean of stimulation index ≤ 1 for $CD4^+$ T cells population; suggesting that $CD4^+$ T cells from infected mice (regardless of treatment) have no detectable TSA-1-C4+Tc24-C4-antigen specific cells. Besides, the stimulation index of antigen-specific $CD8^+$ T cells from all groups had a mean of stimulation index ≥ 1 (**S5 Fig**), confirming the presence of TSA-1-C4+Tc24-C4-antigen specific cells in *T. cruzi*-infected mice at the late chronic phase. These results suggest that during the late chronic phase there are antigen specific $CD8^+$ T cells in all infected groups that can be recalled using antigen presenting cells (APC) such as macrophages. However, at 200 days p.i., we did not find differences among groups for antigen-specific $CD4^+$ or $CD8^+$ T cells (ANOVA, P=0.858 and P=0.793 respectively).

To evaluate the intracellular IFNγ and perforin production by TSA-1-C4+Tc24-C4-antigen-specific $CD4^+$ and $CD8^+$ T cells, mononuclear cells were isolated and co-cultivated with antigen-specific RAW 264.7 macrophages, as described before. According to **Fig 5A,** we observed that $CD4^+$ T cells from the low BNZ + vaccine treated mice showed a significantly higher production of IFNγ (1.056 ± 0.062), compared to E6020-SE (0.958 ± 0.023) or low BNZ alone (0.954 ± 0.06) treated groups (Student´s t-test, P=0.002 and P=0.007 respectively). On the other hand, mice treated with the vaccine alone (1.367 ± 0.504) or the combination low BNZ + vaccine (1.089 ± 0.572) had the highest production of perforin by antigen-specific $CD4^+$ T cells (**Fig 5B**) and were significantly higher when comparing with infected untreated mice (0.532 ± 0.359) (Mann-Whitney U test, P=0.002 and P=0.049 respectively).

Fig 5. Effect of vaccine-linked chemotherapy on antigen-specific CD4$^+$ and CD8$^+$ T cells functional profile. Mononuclear cells isolated from mice at 200 days p.i were co-cultivated with macrophages stimulated *in vitro* with TSA-1-C4+Tc24-C4 (25 μg/mL) for 20 h. Data were analysed using FlowJo X software. Stimulation index of (**A**) antigen-specific IFNγ-producing CD4$^+$ cells, (**B**) perforin-producing CD4$^+$ cells, (**C**) IFNγ-producing CD8$^+$ cells and (**D**) perforin-producing CD8$^+$ cells are presented. Each point represents an individual mouse, horizontal lines denote means ± SD or median ± interquartile ranges values according to the normality of the data. Data were analysed using Student´s t-test or Mann-Whitney U-test. Significance is indicated as follows *, $P \leq 0.05$; **, $P \leq 0.01$.

For antigen-specific CD8$^+$ T cells, we observed a cytotoxic immuno-phenotype profile characterized by higher perforin-producing CD8$^+$ T cells in low BNZ + vaccine treated mice (**Fig 5D**), (1.567 ± 0.728) compared to the infected untreated group (0.838 ± 0.386) or the low BNZ treated group (0.699 ± 0.570) (Student´s t-test, $P=0.025$ and $P=0.018$ respectively), however, no differences were found when we evaluate the production of IFNγ by CD8$^+$ T cells (**Fig 5C**). All these findings suggest that the vaccine-linked chemotherapy might ameliorate the fibrosis in *T. cruzi* chronic infection by induction of a TSA-1-C4+Tc24-C4-antigen specific CD4$^+$ and CD8$^+$ cytotoxic T cells with a perforin-phenotype and these can be recalled up to day 200 p.i. in our mouse model.

Treatment given during early chronic infection induced a long-lasting *T. cruzi*-immunity

With the purpose to evaluate the memory T cell profile induced by the vaccine-linked chemotherapy, we measured markers of central (T_{CM}) ($CD44^+CD62L^+$) and effector (T_{EM}) ($CD44^+CD62L^-$) T cell memory subpopulation in $CD4^+$ and $CD8^+$ T cells.

As observed in **Fig 6A**, we found a significantly higher stimulation index of antigen-specific $CD4^+$ T_{CM} sub-population in the low BNZ + vaccine treated mice (1.19 ± 0.073) and vaccine alone groups (1.206 ± 0.105) compared to infected untreated mice (1.085 ± 0.07) (Student´s t-test, P=0.026 and P=0.018 respectively). Similarly, a significantly higher stimulation index of $CD8^+$ T_{CM} sub-population (**Fig 6B**), was observed in low BNZ + vaccine treated mice (1.485 ± 0.519) and vaccine alone groups (1.33 ± 0.18) compared to infected untreated mice (0.995 ± 0.149) (Student´s t-test, P=0.032 and P=0.002 respectively). Otherwise, we observed that low BNZ + vaccine treated mice (0.808± 0.054) and low BNZ alone treatment (0.808 ± 0.07) had lower stimulation index of antigen-specific $CD4^+$ T_{EM} sub-population compared to infected untreated mice (0.908 ± 0.076) (Student´s t-test, P=0.012 and P=0.02 respectively) **Fig 6C**. Finally, there was no difference in $CD8^+$ T_{EM} at late chronic infection (200 days p.i.) (**Fig6 D**). Of note, the vaccine alone or linked-chemotherapy elicited TSA-1-C4+Tc24-C4 antigen-specific central memory response during the late chronic phase of *T. cruzi*-infection in BALB/c mice.

Fig 6. Effect of vaccine-linked chemotherapy on antigen-specific $CD4^+$ and $CD8^+$ T cells memory response. Mononuclear cells isolated from mice at 200 days p.i. were co-cultivated with macrophages stimulated *in vitro* with TSA-1-C4+Tc24-C4 (25 µg/mL) for 96 h. Data were analysed using FlowJo X software. Stimulation index of antigen-specific (**A**) $CD4^+$ Central Memory, (**B**) $CD4^+$ Effector Memory, (**C**) $CD8^+$ Central Memory and (**D**) $CD8^+$

449 Effector Memory T cells are presented. Each point represents an individual mouse, horizontal
450 lines denote mean ± SD values, and data were analysed using Student´s t-test. Significance
451 is indicated as follows *, $P \leq 0.05$.

452

453

454 Discussion

455 One of the greatest challenges in chronic CD is the development of therapies that improve
456 prognosis and, even, reverse the cardiac injury. Our research partnership is developing a
457 therapeutic vaccine against CD that seeks to prevent or delay the onset of CCC in infected
458 patients. Previous studies by our group have evidenced the feasibility of DNA vaccines
459 formulated with TSA-1 and Tc24 *T. cruzi*-antigens in mice and dogs (33,50,51). This DNA-
460 bivalent vaccine was associated with a $CD8^+$ T cell activity, IFNγ production, Th1 immune
461 response. Since DNA vaccines historically have not been yet progressed successfully to
462 emergency use authorization or full licensure for use in humans, our studies have focused on
463 recombinant protein antigens (52). Hence, we embarked on studies to evaluate vaccines
464 formulated with TSA-1 or Tc24 recombinant proteins in conjunction with Toll-like receptor
465 4 agonist adjuvants (30,47). These previous studies have concluded that either Th1 or
466 balanced Th1/Th2 immune responses are associated with reductions in parasite burdens,
467 fibrosis, and host infiltrating inflammation linking it to confer protection in experimental
468 models of acute *T. cruzi* infection (16,31,32).

469 Specific genetic mutations have been made for both recombinant proteins, to facilitate
470 production and increase stability, while maintaining immunogenicity in mice; the proteins
471 resulting were named as TSA-1-C4 and Tc24-C4 (28,29). These designations reflect the
472 modification of cysteines to prevent protein aggregation from intermolecular disulphide bond
473 formation. The bivalent vaccine, therefore, is comprised of two recombinant *T. cruzi*
474 antigens, Tc24-C4 and TSA-1-C4, demonstrated immunogenicity in non-human primate
475 trials study (53). An effective therapeutic treatment for CD must prove its effectiveness at
476 preventing or delaying the onset of CCC (17). Thereby, it is critical to evaluate therapeutic
477 treatments in pre-clinical models during the chronic phase of *T. cruzi*-infection. Recently,
478 studies aimed to evaluate BNZ in reduced dosing regimens to decreasing adverse side-effects
479 (39,41). Here, we evaluated the therapeutic efficacy of a vaccine candidate formulated with
480 TSA-1-C4 + Tc24-C4 recombinant antigens combined with a 4-fold reduction in the amount
481 and dosage regimen of BNZ treatment given during the early chronic phase of *T. cruzi*-
482 infection in a murine model and followed until the late chronic phase of the disease.

483 In terms of protective effect, a diminished parasitemia and cardiac parasite burdens
484 are related with therapeutic efficacy in murine models of *T. cruzi* acute infection
485 (15,31,32,42,47). On the other hand, *T. cruzi* parasites in blood and cardiac tissue decrease
486 with time during *T. cruzi* chronic infection becoming undetectable in blood and restricted in
487 tissues, where they are not always demonstrable, even by using highly sensitive amplification
488 techniques as qPCR assay (54). However, novel techniques using a bioluminescence imaging
489 system have allowed to measure the burden parasite *in vivo* during *T. cruzi*-chronic infection
490 demonstrating that the *T. cruzi* presence in the heart is spatially dynamic (55). This finding
491 suggests that parasitemia, as well as cardiac parasite burden alone, are not robust indicators

492 to evaluate therapeutic efficacy during *T. cruzi* chronic infection in murine models.
493 Therefore, the absence of detectable parasites in the heart at a point of infection does not
494 necessarily exclude the ongoing infection itself, as the parasite could be restricted to other
495 organs, such as in the gastrointestinal tract (55). This could explain our results, as we detected
496 low levels of parasite burden in the heart. Further studies need to be performed in order to
497 understand the mechanism that allows the establishment of cardiac disease in irregular levels
498 of parasites.

499 Beyond parasite reduction, there are findings stressing the role of reducing both
500 cardiac fibrosis and inflammation in patients, non-human primates and mice (56,57). In fact,
501 the use of non-invasive methods to measure fibrosis have allowed to distinguish potentially
502 useful biomarkers of cardiac fibrosis, such as TGF-β, connective tissue growth factor, and
503 platelet-derived growth factor-D (48). In the current study, we showed that infected untreated
504 mice in chronic infection exhibited a more severe cardiac fibrosis compared to the non-
505 infected control group, as expected. Also, we observed that the vaccine-linked
506 chemotherapy-treated group had on average only 50% of the cardiac fibrosis area compared
507 to infected untreated group. Thus, we demonstrated that the vaccine-linked chemotherapy
508 given at the early chronic phase of *T. cruzi* infection is able to prevent cardiac fibrosis in our
509 mouse model. In this experimental infection model, the administration of the low dose of
510 BNZ alone (25mg/kg for 7 days) is unable to prevent cardiac fibrosis at 200 days p.i. These
511 results coincide with previous studies, showing that BNZ therapy (100mg/kg for 20 days)
512 prevents the development of cardiac fibrosis in the murine model when treatment is
513 administrated in the acute phase however, the drug fails when is administrated during the
514 chronic phase of infection (58).

Our findings support previous studies in mice during acute infection by *T. cruzi* showing that Tc24 and Tc24-C4 immunizations or the vaccine-linked chemotherapy can reduce parasite burden, cardiac fibrosis, and inflammation (15,16,32,42). In addition, we confirmed that the protective effect is provide for the antigens and it is not due to adjuvant. For instance, we have previously evaluated the dose-response effect of E6020-SE administration on cardiac fibrosis using a lethal acute infection murine model (59). According to our previous findings, E6020-SE administration alone does not prevent cardiac fibrosis development during acute phase. Here, we showed that mice treated with 5 µg of E6020-SE alone during the early chronic infection, still develop cardiac fibrosis at the late chronic phase of *T. cruzi*-infection. Therefore, our results suggest that the vaccine antigen component is necessary to achieve optimal protection against cardiac fibrosis development.

As part of the study, we evaluated protection against cardiac inflammation conferred by our vaccine-linked chemotherapy. According to our data, no significant differences were observed when we compared our vaccine-linked chemotherapy-treated group with the infected untreated group. However, we observed similar levels of inflammatory infiltrate in cardiac tissue from infected untreated and non-infected mice suggesting that the percentage of inflammation in cardiac tissue from infected mice decrease over the course of infection until reach basal levels on late chronic stages of the disease (200 days p.i), as has been previously described by Hoffman (48).

The $CD8^+$ cytotoxic T cells activation is essential to achieve immunity against *T. cruzi* as well other parasites (60,61). We showed that the vaccine-linked chemotherapy-treated group had on average double production of perforin by antigen-specific $CD8^+$ T cells compared to infected untreated mice. Our results pointed out that the immunotherapy with

538 TSA-1-C4+Tc24-C4 recombinant antigens is able to prime a cytotoxic profile ($CD8^+Perf^+$)
539 during the late chronic phase of *T. cruzi*-infection. Also, vaccine-linked chemotherapy
540 elicited an antigen-specific $CD4^+$ CTL sub-population, these cells can secrete cytotoxic
541 granules that directly kill infected cells in an MHC-class-II-restricted context. Previous
542 studies have described $CD4^+$ CTL sub-population in both, human and murine models (62–
543 64). Currently, the mechanism used by $CD4^+$ CTL is unclear, however; this sub-population
544 can exhibit functions complementary to $CD8^+$ CTLs (65). More studies are needed to
545 elucidate the role of $CD4^+$ CTL in *T. cruzi* infection.

546 On the other hand, we did not observe significant differences neither antigen-
547 specific $CD4^+IFN\gamma^+$ nor $CD8^+IFN\gamma^+$-producing T cells in the vaccine-linked chemotherapy-
548 treated mice compared with the infected untreated group. Both phenotypes are characteristic
549 of the Th1 immune response that is known to confer protection against *T. cruzi* acute
550 infection. We believe that this finding is consistent with the chronic phase of infection since
551 parasitemia has been controlled as well as cardiac parasite burden in both infected mice
552 groups. Therefore, it is unlikely to observe the activation of TSA-1-C4 or Tc24-C4 antigen-
553 specific $CD4^+IFN\gamma^+$ or $CD8^+IFN\gamma^+$ T cells populations in the spleen of mice that have already
554 controlled the infection.

555 A challenge in the development of an effective vaccine against *T. cruzi* is the
556 induction of long-lived memory cells, which confers long-term protection. In our study, we
557 were able to recall antigen-specific $CD4^+$ and $CD8^+$ T_{CM} sub-populations at 200 days p.i. The
558 central memory T cells are distinguished for having a proliferative response followed by
559 antigenic stimulation that live longer than effector memory cells. Bixby and Tarleton have
560 previously reported during *T. cruzi*-infection in mice this sub-population in $CD8^+$ T cells

561 showing distinctive features called as T_{CM} cells (36). Similarly, T_{EM} sub-population
562 represents a type of terminally differentiated cells that produce IFNγ and IL-4 or contain
563 prestored perforin (34). In this study, we observed a low proportion of either $CD4^+$ or $CD8^+$
564 T_{EM} sub-populations regardless of treatment from infected mice at 200 days p.i probably as
565 consequence that effector cells are characterized by requiring a continuous antigen
566 presentation by APC in order to proliferate and differentiate. We suggested that during the
567 first weeks after the vaccine administration, T_{EM} sub-populations have differentiated and
568 performed their effector activity, preventing the dissemination of the parasite, and ensuring
569 the survival of the mice. This may explain the low levels of load parasite load observed by
570 qPCR at day 200 p.i. Thus, we propose that for this experimental infection model, during the
571 late chronic phase, the immune system remains in a "resting-state", in which there is a limited
572 effector activity. However, the use of the recombinant-protein vaccine recalls a strong central
573 memory response mediated by antigen-specific T cells at 200 days p.i. In sum, our results
574 suggest that a TSA-1-C4+Tc24-C4 antigen-specific T central memory sub-population could
575 protect against reinfection during late chronic *T. cruzi* infection in our murine model.

576 There are some limitations in this study. We did not measure clinical parameters to
577 assess heart function. Therefore, we were not able to correlate the reduced fibrosis with
578 improved clinical cardiac output in our chronically infected mice. In addition, the BALB/c
579 model of experimental infection used here seems to have an intrinsic resistance to *T. cruzi*
580 acute infection allowing them to progress until the late chronic phase, which is characterized
581 by lower levels of parasite burden and inflammation but higher percentages of cardiac
582 fibrosis in infected untreated mice. However, our BALB/c model may be representative of a

583 majority proportion of the *T. cruzi* infected human population that has the ability to control
584 parasite burden and inflammation, remaining in asymptomatic chronic phase of CD for life.

585

586

587 Conclusion

588 We demonstrate that treatment with a low dose BNZ and a vaccine immunotherapy protects
589 mice against cardiac fibrosis progression and induces a long-lasting *T. cruzi*-immunity that
590 persists for at least 18 weeks post-treatment. This study supports the use of a vaccine-linked
591 chemotherapy approach given in early chronic infection, however; additional studies in other
592 preclinical models that develop CCC and with more characteristics of human disease, such
593 as non-human primates, will be necessary before the combination of a vaccine-linked to BNZ
594 can be moved into clinical trials.

595

596

597 Supporting information

598 **S1 Table. Parasitemia measurement.** A total of 70 BALB/c mice were infected with 500
599 trypomastigotes of *T. cruzi* (H1 strain) by intraperitoneal injection. A total of 4 mice were
600 used as non-infected control group and received only saline solution. Parasitemia was
601 measured in Neubauer chamber by examination of fresh blood collected from the mouse tail
602 at day 27 post-infection. All mice who received infection were positive for *T. cruzi*, while

603 neither mouse from non-infected control group were reported as positive. **SD**, standard
604 deviation; **CI**, confidence interval.

605 **S1 Fig. protein integrity assessment.** SDS-PAGE analysis at 12% of acrylamide/bis-
606 acrylamide and stain with PageBlue™ Protein Staining Solution (ThermoFisher
607 Scientific®). Molecular weight marker (Spectra™ Multicolor Broad Range Protein Ladder
608 from ThermoFisher Scientific®) and recombinant proteins TSA-1-C4 (65 kDA) and Tc24-
609 C4 (24 kDa) are presented.

610 **S2 Fig. Survival curve.** A total of 70 BALB/c mice were infected with 500 trypomastigotes
611 of *T. cruzi* (H1 strain) by intraperitoneal injection. A total of 4 mice were used as non-infected
612 control group and received only saline solution. Survival was monitored during 200 days
613 post-infection.

614 **S3 Fig. Flow-cytometry gating strategy for IFNγ and perforin production.** The dot-plots
615 show the mononuclear cells gating based on (**A**) forward-scatter (FSC) and side-scatter (SSC)
616 properties, (**B**) doublets exclusion, (**C**) identification of $CD3^+$ positive cells, (**D**) phenotype
617 of $CD4^+$ and $CD8^+$ cells and (**E**) IFNγ and perforin expression. Gates were stablished based
618 on FMO controls corresponding to each antibody.

619 **S4 Fig. Flow-cytometry gating strategy for central and effector memory response.** The
620 dot-plots show the mononuclear cells gating based on (**A**) forward-scatter (FSC) and side-
621 scatter (SSC) properties, (**B**) doublets exclusion, (**C**) identification of CD3 positive cells, (**D**)
622 phenotype of $CD4^+$ and $CD8^+$ cells and (**E**) central memory and effector memory profile
623 defined by ($CD44^+CD62L^+$) and ($CD44^+CD62L^-$) expression respectively. Gates were
624 established based on FMO controls corresponding to each antibody.

S5 Fig. Effect of vaccine-linked chemotherapy on antigen-specific total CD4$^+$ and CD8$^+$ T cells response. Mononuclear cells isolated from mice at 200 days post-infection were co-cultivated with macrophages stimulated in vitro with TSA-1-C4+Tc24-C4 (25 μg/mL) for 20 h. Data were analysed using FlowJo X software. Stimulation index of antigen-specific (**A**) CD4$^+$ cells and (**B**) CD8$^+$ cells are presented. Each point represents an individual mouse, data were analysed using ANOVA for multiple comparisons.

Author contributions

Conceptualization: Dumonteil E, Cruz-Chan J.V and Villanueva-Lizama L.E

Data curation: Dzul-Huchim V.M and Villanueva-Lizama L.E

Formal analysis: Dzul-Huchim V.M, Cruz-Chan J.V and Villanueva-Lizama L.E

Funding acquisition: Rosado-Vallado M.E, Hotez P and Bottazzi M.E

Investigation: Dzul-Huchim V.M and Villanueva-Lizama L.E

Methodology: Dzul-Huchim V.M, Arana-Argaez V.E, Dumonteil E and Villanueva-Lizama L.E

Project administration: Hotez P, Bottazzi M.E and Villanueva-Lizama L.E

Resources: Ramirez-Sierra M.J, Martinez-Vega PB, Ortega-Lopez J and Gusovsky F

643 **Supervision:** Rosado-Vallado M.E, Cruz-Chan J.V, Villanueva-Lizama L.E, Hotez P and
644 Bottazzi M.E

645 **Visualization:** Dzul-Huchim V.M and Villanueva-Lizama L.E

646 **Writing – original draft:** Dzul-Huchim V.M

647 **Writing – review & editing:** Arana-Argaez V.E, Cruz-Chan J.V, Villanueva-Lizama L.E,
648 Ortega-Lopez J, Gusovsky F, Hotez P and Bottazzi M.E

649

650

651 # References

652 **1.** World Health Organization. Chagas disease (American trypanosomiasis)- Global
653 distribution of cases of Chagas disease based on official stimates on 2018. Available
654 from: https://www.who.int/health-topics/chagas-disease#tab=tab_1
655 **2.** Hotez PJ, Basáñez MG, Acosta-Serrano A, Grillet ME. Venezuela and its rising vector-
656 borne neglected diseases. PLoS Negl Trop Dis. 2017; 29;11(6):e0005423.
657 doi:10.1371/journal.pntd.0005423 PMID: 28662038
658 **3.** Laranja FS, Dias E, Nobrega G, Miranda A. Chagas' disease; a clinical, epidemiologic,
659 and pathologic study. J. Am. Heart. Assoc. 1956; 14(6),1035–1060.
660 doi:10.1161/01.CIR.14.6.1035 PMID: 13383798
661 **4.** Rassi Jr A, Rassi A, Marin-Neto J. Chagas disease. Lancet. 2010; 375,(9723)1388–1402.
662 doi:10.1016/S0140-6736(10)60061-X PMID: 20399979
663 **5.** Teixeira M, Gazzinelli R, Silva J. Chemokines, inflammation and *Trypanosoma cruzi*

664 infection. Trends Parasitol. 2002; 18(6),262–265. doi:10.1016/s1471-4922(02)02283-3
665 PMID: 12036740

666 **6.** Ribeiro AL, Nunes MP, Teixeira MM, Rocha MOC. Diagnosis and management of
667 Chagas disease and cardiomyopathy. Nat. Rev. Cardiol. 2012; 9(10),576–589.
668 doi:10.1038/nrcardio.2012.109 PMID: 22847166

669 **7.** Ramírez JD, Guhl F, Rendón LM, Rosas F, Marin-Neto, JA, Morillo CA. Chagas
670 cardiomyopathy manifestations and *Trypanosoma cruzi* genotypes circulating in chronic
671 chagasic patients. PLoS Negl Trop Dis. 2010; 4(11),e899.
672 doi:10.1371/journal.pntd.0000899 PMID: 21152056

673 **8.** Nevers T, Salvador AM, Velazquez F, Ngwenyama N, Carrillo-Salinas FJ, Aronovitz M,
674 et al. Th1 effector T cells selectively orchestrate cardiac fibrosis in nonischemic heart
675 failure. J Exp Med 2017; 214(11),3311–3329. doi:10.1084/jem.20161791 PMID:
676 28970239

677 **9.** Viotti R, Vigliano C, Lococo B, Alvarez MG, Petti M, Bertocchi G, et al. Side effects of
678 benznidazole as treatment in chronic Chagas disease: Fears and realities. Expert Rev Anti
679 Infect Ther. 2009; 7(2),157–163. doi:10.1586/14787210.7.2.157 PMID: 19254164

680 **10.** Morillo CA, Marin-Neto JA, Avezum A, Sosa-Estani S, Rassi A, Rosas F, et al.
681 Randomized trial of benznidazole for chronic Chagas' cardiomyopathy. N Engl J Med.
682 2015; 373(14),1295–1306. doi:10.1056/NEJMoa1507574 PMID: 26323937

683 **11.** Viotti R, Vigliano C, Lococo B, Bertocchi G, Petti M, Alvarez MG, et al. Long-term
684 cardiac outcomes of treating chronic Chagas disease with benznidazole versus no
685 treatment: a nonrandomized trial. Ann. Intern. Med. 2006; 144(10),724–34.
686 doi:10.7326/0003-4819-144-10-200605160-00006 PMID: 16702588

687 **12.** Limon-Flores A, Cervera-Cetina R, Tzec-Arjona J, Ek-Macias L, Sanchez-Burgos G,

688 Ramirez-Sierra MJ, et al. Effect of a combination DNA vaccine for the prevention and
689 therapy of *Trypanosoma cruzi* infection in mice: Role of $CD4^+$ and $CD8^+$ T cells.
690 Vaccine. 2010; 28(46),7414–7419. doi:10.1016/j.vaccine.2010.08.104 PMID: 20850536
691 **13.** Pereira IR, Vilar-Pereira G, Marques V, da Silva A, Caetano B, Moreira OC, et al. A
692 human type 5 adenovirus-based *Trypanosoma cruzi* therapeutic vaccine re-programs
693 immune response and reverses chronic cardiomyopathy. PLoS Pathog. 2015;
694 11(1),e1004594. doi:10.1371/journal.ppat.1004594 PMID: 25617628
695 **14.** Teh-Poot C, Tzec-Arjona E, Martínez-Vega PP, Ramirez-Sierra MJ, Rosado-Vallado M,
696 Dumonteil E. From genome screening to creation of vaccine against *Trypanosoma cruzi*
697 by use of immunoinformatics. J Infect Dis. 2015; 211(2),258–266.
698 doi:10.1093/infdis/jiu418 PMID: 25070943
699 **15.** Barry MA, Wang Q, Jones KM, Heffernan MJ, Buhaya H, Beaumier CM, et al. A
700 therapeutic nanoparticle vaccine against *Trypanosoma cruzi* in a BALB/c mouse model
701 of Chagas disease. Hum Vaccin Immunother. 2016; 12(4),976–987.
702 doi:10.1080/21645515.2015.1119346 PMID: 26890466
703 **16.** Barry MA, Versteeg L, Wang Q, PolletJ, Zhan B, Gusovsky F, et al. A therapeutic
704 vaccine prototype induces protective immunity and reduces cardiac fibrosis in a mouse
705 model of chronic *Trypanosoma cruzi* infection. PLoS Negl Trop Dis. 2019;
706 13(5),e0007413. doi:10.1371/journal.pntd.0007413 PMID: 31145733
707 **17.** Dumonteil E, Bottazzi ME, Zhan B, Heffernan MJ, Jones K, Valenzuela JG, et al.
708 Accelerating the development of a therapeutic vaccine for human Chagas disease:
709 rationale and prospects. Expert Rev Vaccines. 2012; 11(9),1043–1055.
710 doi:10.1586/erv.12.85 PMID: 23151163
711 **18.** Bivona AE, Sánchez-Alberti A, Cerny N, Trinitario SN, Malchiodi EL. Chagas disease

712 vaccine design: the search of an efficient *Trypanosoma cruzi* immune-mediated control.
713 Biochim Biophys Acta Mol Basis Dis. 2019; 1;1866(5),165658.
714 doi:10.1016/j.bbadis.2019.165658 PMID: 31904415

715 **19.** Dumonteil E, Herrera C. The case for the development of a Chagas disease vaccine:
716 Why? How? When? Trop Med Infect Dis. 2021; 6(1),16.
717 doi:10.3390/tropicalmed6010016 PMID: 33530605

718 **20.** Martin D, Tarleton R. Generation, specificity, and function of $CD8^+$ T cells in
719 *Trypanosoma cruzi* infection. Immunol Rev. 2004; 201,304–17. doi:10.1111/j.0105-
720 2896.2004.00183.x PMID: 15361249

721 **21.** Tarleton RL. $CD8^+$ T cells in *Trypanosoma cruzi* infection. Semin. Immunopathol. 2015;
722 37(3),233–8. doi:10.1007/s00281-015-0481-9 PMID: 25921214

723 **22.** Padilla AM, Bustamante JM, Tarleton RL. $CD8^+$ T cells in *Trypanosoma cruzi* infection.
724 Curr Opin Immunol. 2009; 21(14),385–90. doi:10.1016/j.coi.2009.07.006 PMID:
725 19646853

726 **23.** Pipkin ME, Lieberman JL. Delivering the kiss of death: progress on understanding how
727 perforin works. Curr Opin Immunol. 2007; 19(3),301–8. doi:10.1016/j.coi.2007.04.011
728 PMID: 17433871

729 **24.** Chowdhury D, Lieberman JL. Death by a thousand cuts: granzime pathways of
730 programmed cell death. Annu Rev Immunol. 2008; 26,389–420.
731 doi:10.1146/annurev.immunol.26.021607.090404 PMID: 18304003

732 **25.** Abrahamsohn IA, Coffmann RL. *Trypanosoma cruzi*: IL-10 , TNFα, IFN-gamma, and
733 IL-12 regulate innate and acquired immunity to infection. Exp Parasitol. 1996;
734 *84*(2),231–244. doi:10.1006/expr.1996.0109 PMID: 8932773

735 **26.** Martins GA, Vieira LQ, Cunha FQ, Silva JS. Gamma interferon modulates CD95 (Fas)

736 and CD95 ligand (Fas-L) expression and nitric oxide-induced apoptosis during the acute
737 phase of *Trypanosoma cruzi* infection: A possible role in immune response control. Infect
738 Immunol. 1999; 67(8),3864–3871. doi:10.1128/iai.67.8.3864-3871.1999 PMID:
739 10417150

740 **27.** Acosta-Rodriguez EV, Araujo-Furlan C, Fiocca-Vernengo F, Montes C, Gruppi A.
741 Understanding $CD8^+$ T cell immunity to *Trypanosoma cruzi* and how to improve it.
742 Trends Parasitol. 2019; 35(11),899–917. doi:10.1016/j.pt.2019.08.006 PMID: 31607632

743 **28.** Seid CA, Jones KM, Pollet J, Keegan B, Hudspeth E, Hammond M, et al. Cysteine
744 mutagenesis improves the production without abrogating antigenicity of a recombinant
745 protein vaccine candidate for human Chagas disease. Hum Vaccin Immunother. 2017;
746 13(3),621–633. doi:10.1080/21645515.2016.1242540 PMID: 27737611

747 **29.** Biter AB, Weltje S, Hudspeth EM, Seid CA, McAtee PC, Chen WH, et al.
748 Characterization and stability of *Trypanosoma cruzi* 24-C4 (Tc24-C4), a candidate
749 antigen for a therapeutic vaccine against Chagas disease. J Pharm Sci. 2018;
750 107(5),1468–73. doi:10.1016/j.xphs.2017.12.014 PMID: 29274820

751 **30.** de la Cruz-Lopez JJ, Villanueva-Lizama LE, Dzul-Huchim VD, Vega-Martinez PB,
752 Ramirez-Sierra MJ, Rosado-Vallado ME, et al. Production of recombinant TSA-1 and
753 evaluation of its potential for the immuno-therapeutic control of *Trypanosoma cruzi*
754 infection in mice. Hum Vaccin Immunother. 2019; 15(1),210–219.
755 doi:10.1080/21645515.2018.1520581 PMID: 30192702

756 **31.** Konduri V, Halpert MM, Liang D, Levitt JM, Cruz-Chan JV, Zhan B, et al. Genetic
757 adjuvantation of a cell-based therapeutic vaccine for amelioration of chagasic
758 cardiomyopathy. Infect Immun. 2017; 85(9),e00127-17. doi:10.1128/IAI.00127-17
759 PMID: 28674032

760 **32.** Jones K, Versteeg L, Damania A, Keegan B, Kendricks A, Pollet J, et al. Vaccine-linked
761 chemotherapy improves benznidazole efficacy for acute Chagas disease. Infect Immun.
762 2018; 86(4),e00876-17. doi:10.1128/IAI.00876-17 PMID: 29311242
763 **33.** Quijano-Hernandez I, Bolio-Gonzalez M, Rodriguez-Buenfil J, Ramirez-Sierra MJ,
764 Dumonteil E. Therapeutic DNA vaccine against *Trypanosoma cruzi* infection in dogs.
765 Ann N Y Acad Sci. 2008; 1149,343–346. doi:10.1196/annals.1428.098 PMID: 19120245
766 **34.** Lanzavecchia A, Sallusto F. Dynamics of T lymphocyte responses: intermidiates,
767 effectors, and memory cells. Science. 2000; 290(5489),92–7.
768 doi:10.1126/science.290.5489.92 PMID: 11021806
769 **35.** Martin D, Tarleton R. Antigen-specific T cells maintain an effector memory phenotype
770 during persistent *Trypanosoma cruzi* infection. J. Immunol. 2005; 174,(3),1594–601.
771 doi:10.4049/jimmunol.174.3.1594 PMID: 15661921
772 **36.** Bixby LM, Tarleton RL. Stable $CD8^+$ T cell memory during persistent *Trypanosoma*
773 *cruzi* infection. J Immunol. 2008; 181(4),2644–2650. doi:10.4049/jimmunol.181.4.2644
774 PMID: 18684955
775 **37.** Bustamante JM, Bixby LM, Tarleton RL. Drug-induced cure drives conversion to a stable
776 and protective $CD8^+$ T central memory response in chronic Chagas disease. Nat Med
777 2008; 14(5),542–50. doi:10.1038/nm1744 PMID: 18425131
778 **38.** Rigatto PO, de Alancar BC, de Vasconcelos JR, Dominguez MR, Araújo AF, Machado
779 AV, et al. Heterologous plasmid DNA prime-recombinant human adenovirus 5 boost
780 vaccination generates a stable pool of protective long-lived $CD8^+$ T effector memory cells
781 specific for a human parasite, *Trypanosoma cruzi*. Infect Immun. 2011; 79(5),2120–30.
782 doi:10.1128/IAI.01190-10 PMID: 21357719
783 **39.** Cencig S, Coltel N, Truyens C, Carlier Y. Evaluation of benznidazole treatment

784 combined with nifurtimox, posaconazole or AmBisome in mice infected with
785 *Trypanosoma cruzi* strains. Int J Antimicrob Agents. 2012; 40(6),527–532.
786 doi:10.1016/j.ijantimicag.2012.08.002 PMID: 23063742
787 **40.** Diniz L, Urbina JA, Mayer de Andrade I, Mazzeti AL, Martins TA, Caldas IS, et al.
788 Benznidazole and posoconazole in experimental Chagas disease: positive interaction in
789 concomitant and sequential treatments. PLOS Negl Trop Dis. 2013; 7(8),e2367.
790 doi:10.1371/journal.pntd.0002367 PMID: 23967360
791 **41.** Bustamante JM, Craft JM, Crowe BD, Ketchie SA, Tarleton RL. New, combined, and
792 reduced dosing treatment protocols cure *Trypanosoma cruzi* infection in mice. J Infect
793 Dis. 2014; 209(1),150–162. doi:10.1093/infdis/jit420 PMID: 23945371
794 **42.** Cruz-Chan JV, Villanueva-Lizama LE, Versteeg L, Damania A, Villar MJ, González-
795 López C, et al. Vaccine-linked chemotherapy induces IL-17 production and reduces
796 cardiac pathology during acute *Trypanosoma cruzi* infection. Sci Rep. 2021; 11(1),3222
797 doi:10.1038/s41598-021-82930-w PMID: 33547365
798 **43.** Ishizaka ST, Hawkins LD. E6020: A synthetic toll-like receptor 4 agonist as a vaccine
799 adjuvant. Expert Rev Vaccines. 2007; 6(5),773–84. doi:10.1586/14760584.6.5.773
800 PMID: 17931157
801 **44.** Dumonteil E, Escobedo-Ortegon J, Reyes-Rodriguez N, Arjona-Torres A, Ramirez-
802 Sierra MJ. Immunotherapy of *Trypanosoma cruzi* infection with DNA vaccines in mice.
803 Infect. Immunol. 2004; 72(1),46–53. doi:10.1128/iai.72.1.46-53.2004 PMID: 14688079
804 **45.** Moser DR, Kirchhoff LV, Donelson JE. Detection of *Trypanosoma cruzi* by DNA
805 amplification using the polymerase chain reaction. J Clin Microbiol. 1989; 27(7),1477–
806 1482. doi:10.1128/JCM.27.7.1477-1482.1989 PMID: 2504769
807 **46.** Cummings KL, Tarleton RL. Rapid quantitation of *Trypanosoma cruzi* in host tissue by

real-time PCR. Mol Biochem Parasitol. 2003; 129(1),53–59. doi:10.1016/S0166-6851(03)00093-8 PMID: 12798506

47. Martinez-Campos TV, Martinez-Vega, PP, Ramirez-Sierra MJ, Rosado-Vallado ME, Seid CA, Hudspeth EM, et al. Expression, purification, immunogenicity, and protective efficacy of a recombinant Tc24 antigen as a vaccine against *Trypanosoma cruzi* infection in mice. Vaccine. 2015; 33(36),4505–4512. doi:10.1016/j.vaccine.2015.07.017 PMID: 26192358

48. Hoffman KA, Reynolds C, Bottazzi ME, Hotez P, Jones K. Improved biomarker and imaging analysis for characterizing progressive cardiac fibrosis in a mouse model of chronic chagasic cardiomyopathy. J Am Heart Assoc. 2019; 8(22),e013365. doi:10.1161/JAHA.119.013365 PMID: 31718442

49. Marinho CR, D´Império-Lima MR, Grisotto MG, Álvarez JM. Influce of acute-phase parasite load on pathology, parasitism, and activation of the immune system at the late chronic phase of Chagas´disease. Infect Immun. 1999; 67(1),308–18. doi:10.1128/IAI.67.1.308-318.1999 PMID: 9864231

50. Zapata-Estrella H, Hummel-Newell C, Sanchez-Burgos G, Escobedo-Ortegon J, Ramirez-Sierra MJ, Arjona-Torres A, et al. Control of *Trypanosoma cruzi* infection and changes in T-cell populations induced by a therapeutic DNA vaccine in mice. Immunol Lett. 2006; 103(2),186–191. doi:10.1016/j.imlet.2005.11.015 PMID: 16378645

51. Sanchez-Burgos G, Mezquita-Vega RG, Escobedo-Ortegon J, Ramirez-Sierra MJ, Arjona-Torres A, Ouaissi A, et al. Comparative evaluation of therapeutic DNA vaccines against *Trypanosoma cruzi* in mice. FEMS Immunol Med Microbiol. 2007; 50(3),333–341. doi:10.1111/j.1574-695X.2007.00251.x PMID: 17521394

52. Barnard RT. Recombinant vaccines: Strategies for candidate discovery and vaccine

delivery. Expert Rev Vaccines. 2010; 9(5),461–463. doi:10.1586/erv.10.48 PMID: 20450319

53. Dumonteil E, Herrera C, Tu W, Goff K, Fahlberg M, Haupt E, et al. Safety and immunogenicity of a recombinant vaccine against *Trypanosoma cruzi* in Rhesus macaques. Vaccine. 2020; 38(29),4584-4591. doi:10.1016/j.vaccine.2020.05.010 PMID: 32417142

54. Pack AD, Collins MH, Rosenberg CS, Tarleton RL. Highly competent, non-exhausted $CD8^+$ T cells continue to tightly control pathogen load throughout chronic *Trypanosoma cruzi* infection. PLoS Pathog. 2018; 14(11),e1007410. doi:10.1371/journal.ppat.1007410 PMID: 30419010

55. Lewis MD, Francisco AF, Jayawardhana S, Langston H, Taylor MC, Kelly JM, et al. Imaging the development of chronic Chagas disease after oral transmission. Sci. Rep. 2018; 8(1),11292. doi:10.1038/s41598-018-29564-7 PMID: 30050153

56. Carvalho CM, Silverio JC, da Silva AA, Pereira RI, Coelho JM, Britto C, et al. Inducible nitric oxide synthase in heart tissue and nitric oxide in serum of *Trypanosoma cruzi*-infected rhesus monkeys: Association with heart injury. PLoS Neg Trop Dis. 2012; 6(5),e1640. doi:10.1371/journal.pntd.0001644 PMID: 22590660

57. Pereira IR, Vilar-Pereira G, da Silva AA, Lannes-Vieira J. Severity of chronic experimental Chagas' heart disease parallels tumour necrosis factor and nitric oxide levels in the serum: Models of mild and severe disease. Mem Inst Oswaldo Cruz. 2014; 109(3),289–298. doi:10.1590/0074-0276140033 PMID: 24937048

58. Francisco AF, Jayawardhana S, Taylor MC, Lewis MD, Kelly JM. Assessing the effectiveness of curative benznidazole treatment in preventing chronic cardiac pathology in experimental models of chagas disease. Antimicrob Agents Chemother. 2018;

62(10),e00832-18. doi:10.1128/AAC.00832-18 PMID: 30082291

59. Villanueva-Lizama LE, Cruz-Chan JV, Versteeg L, Teh-Pot, C, Hoffmann K, Kendricks A, et al. TLR4 agonist protects against *Trypanosoma cruzi* acute lethal infection by decreasing cardiac parasite burdens. Parasite Immunol. 2020; 42(10),e12769. doi:10.1111/pim.12769 PMID: 32592180

60. Kumar S, Tarleton RL. The relative contribution of antibody production and $CD8^+$ T cell function to immune control of *Trypanosoma cruzi*. Parasite. Immunol. 1998; 20(5),207–216. doi:10.1046/j.1365-3024.1998.00154.x PMID: 9651921

61. de Alencar BCG, Persechini PM, Haolla FA, de Oliveira G, Silverio JC, Lannes-Vieira J, et al. Perforin and gamma interferon expression are required for $CD4^+$ and $CD8^+$ T-cell-dependent protective immunity against a human parasite, *Trypanosoma cruzi*, elicited by heterologous plasmid DNA prime-recombinant adenovirus 5 boost vaccination. Infect. Immunol. 2009; 77(10),4383–4395. doi:10.1128/IAI.01459-08 PMID: 19651871

62. Lukacher AE, Morrison LA, Braciale VL, Malissen B, Braciale TJ. Expression of specific cytolityc activity by H-21 region-stricted, influenza virus-specific T lymphocytes clones. J Exp Med. 1985; 162(1),171–187. doi:10.1084/jem.162.1.171 PMID: 2409206

63. van Leeuwen EM, Remmerswaal EB, Vossen MT, Rowshani AT, Wertheim-van Dillen PM, van Lier RA, et al. Emergence of a $CD4^+$ CD28- granzyme B^+, cytomegalovirus-specific T Cell subset after recovery of primary cytomegalovirus infection. J Immunol. 2004; 173(3),1834–1841. doi:10.4049/jimmunol.173.3.1834 PMID: 15265915

64. Zaunders JJ, Dyer WB, Wang B, Munier ML, Miranda-Saksena M, Newton R, et al. Identification of circulating antigen-specific $CD4^+$ T lymphocytes with a $CCR5^+$, cytotoxic phenotype in an HIV-1 long-term nonprogressor and in CMV infection. Blood.

880 2004; 103(6),2238–2247. doi:10.1182/blood-2003-08-2765 PMID: 14645006

881 **65.** Takeuchi A, Saito T. CD4 CTL, a cytotoxic subset of CD4$^+$ T cells, their differentiation

882 and function. Front Immunol. 2017; 8(194),1–7. doi:10.3389/fimmu.2017.00194 PMID:

883 28280496

884 **Figure 1:**

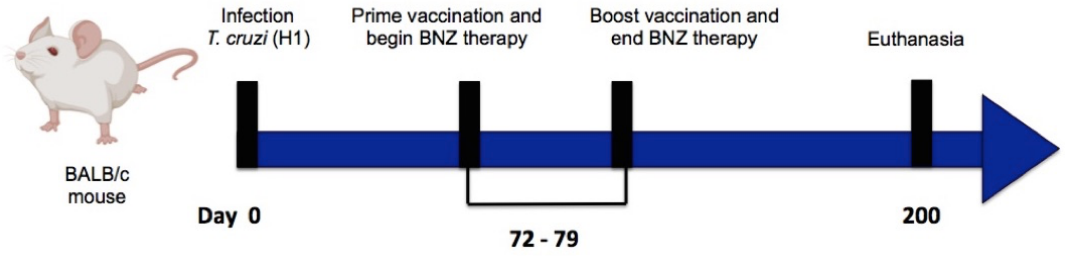

885

886 **Figure 2:**

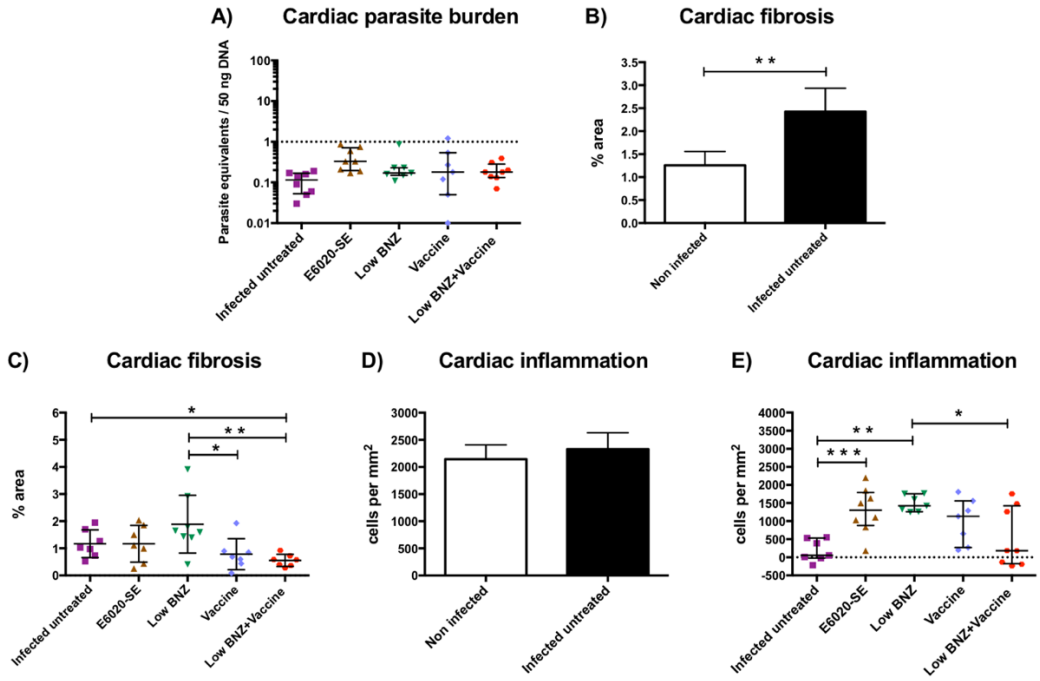

887

888 **Figure 3:**

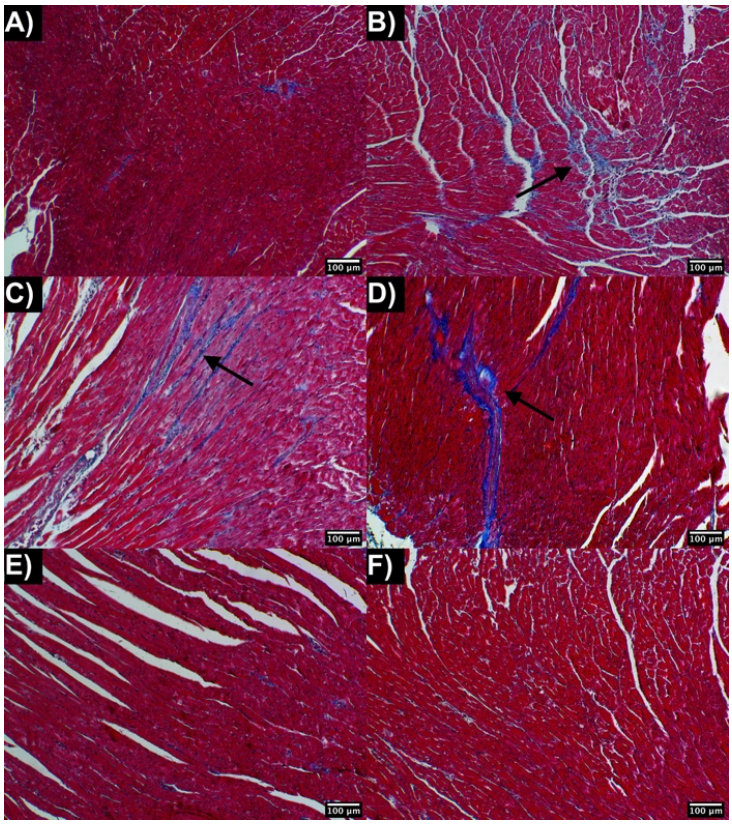

Figure 4:

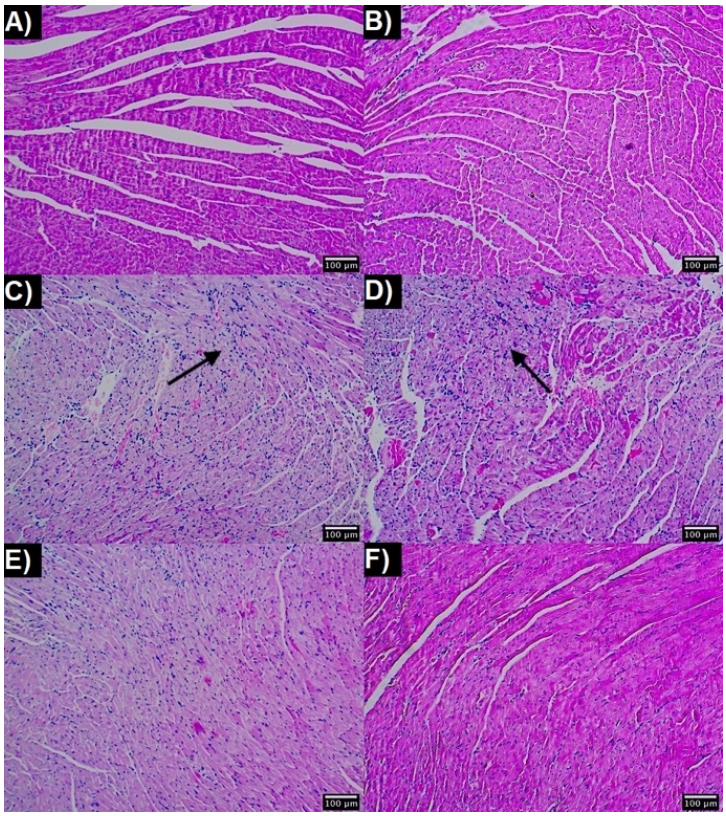

891

892 **Figure 5:**

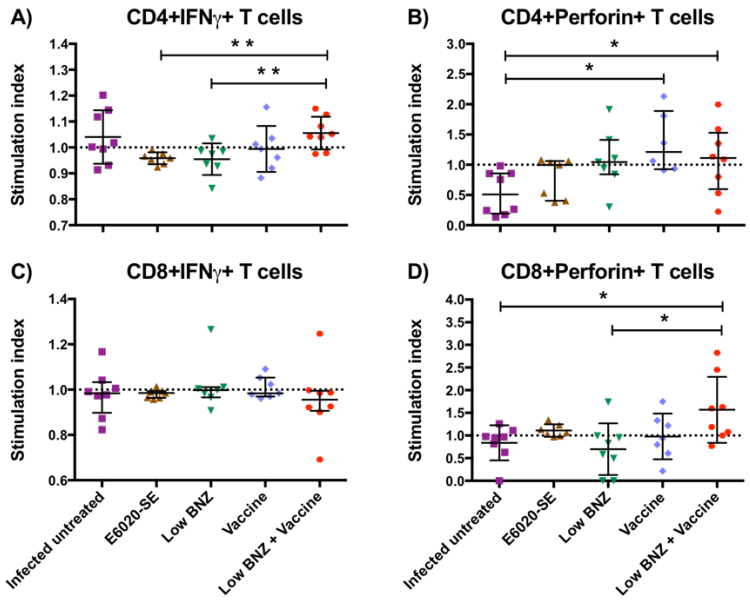

893

894 **Figure 6:**

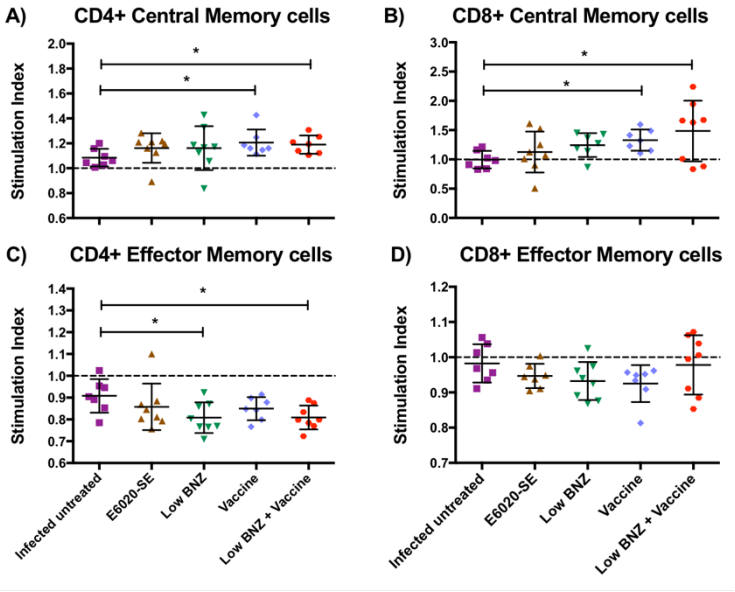

895